Light emission from rough tunnel junctions in UHV

1994 J. Phys.: Condens. Matter 6 9659

(http://iopscience.iop.org/0953-8984/6/45/015)

J. Phys.: Condens. Matter 6 (1994) 9659–9676. Printed in the UK

Light emission from rough tunnel junctions in UHV

M Hänisch and A Otto

Lehrstuhl für Oberflächenwissenschaft (IPkM), Heinrich-Heine-Universität Düsseldorf, 40225 Düsseldorf, Germany

Received 19 May 1994, in final form 4 August 1994

Abstract. Light on both sides of Al–Al_2O_3–Ag junctions is emitted only by the fast surface plasmon polariton mode. The intensity integrated over the spectral distribution and normalized with respect to the tunnel current is about 30 times higher at positive bias (electrons tunnelling into Ag). The explanation of this difference by Kirtley *et al*'s model of excitation of the fast mode by hot electrons is corroborated by 'O quenching' of the emission only at positive bias without a change of the optical reflectivity.

We postulate increased hot-electron–photon coupling within the inhomogeneous electron gas at sites of atomic-scale surface roughness.

1. Introduction

Since the discovery that metal–insulator–metal (MIM, e.g. Ag, Au–Al_2O_3–Al) contacts emit light under appropriate bias in the visible range [2], many publications have dealt with the problem of how this light was generated. The common opinion is that the main part of the light is caused by the scattering of surface plasmon polaritons (SPPs), excited by the tunnelling electrons, into photons. This is supported by the fact that surface roughness increases the photon emission efficiency. Tunnel junctions prepared on a 120 nm thick, rough CaF_2 film emit about 18 times the intensity as a smooth junction [3].

However, there is disagreement about two points at least:

(i) which of the surface plasmon polariton modes deexcites into light and
(ii) which of the surface plasmon polariton modes are excited by the tunnelling electrons.

Three SPP modes of an MIM contact are under discussion as candidates for generation of the observed light. The different modes are characterized by the positions of the maxima of their electric fields at the different boundaries (see figure 1) and by their phase velocities. The SPP with peak field strength in the insulator has a much lower phase velocity than light in Al_2O_3 and is called the slow mode. The SPP with peak strength at the noble metal–air (vacuum) surface has a phase velocity slightly slower than the light velocity in vacuum; hence it is called the fast mode. For exact information on the surface modes of MIM contacts see the calculations in [4]–[8].

Light emission from a mode with maximum intensity at the outside Al interface was observed by Pierce *et al* [9] and Suzuki *et al* [10] with tunnel junctions prepared on a prism coupler with an intermediate film of low index of refraction between prism and Al, which allowed outcoupling of this mode. To our knowledge, there is no report of light emission of the intermediate mode at the CaF_2–Al interface without or with a prism but without an intermediate low-index film.

0953-8984/94/459659+18$19.50

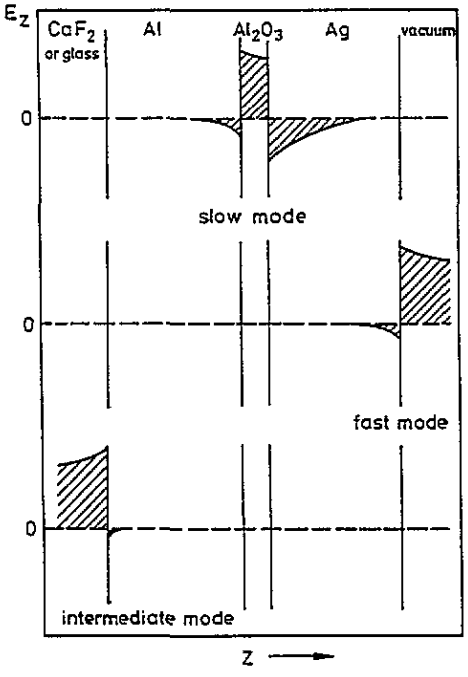

Figure 1. The schematic dependence of the z components of the electric field E on z for the slow, *fast and intermediate* SPP *modes. z is the direction* perpendicular to the stratified layers.

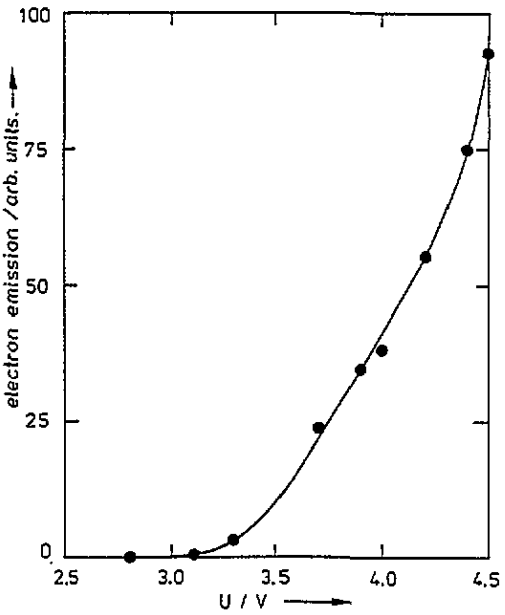

Figure 2. The emission of electrons into the vacuum of tunnel junctions with an Ag top electrode. For an *estimation of the ratio between emitted and tunnelling* electrons multiply by 1.6×10^{-16}. Note that the applied voltages are below the work function of Ag.

The spectral dependence of the emitted light of MIM contacts prepared on CaF_2-covered substrates with Au or Cu top electrodes corresponds to the typical optical absorption structures of Au or Cu (see figures 19 and 20). Dawson *et al* [11] measured the emission of an Au contact to the Al and Au sides and observed no change in the spectral distribution; however, the intensity to the Al side was lower. McCarthy and Lambe [3] prepared smooth Au–Al_2O_3–Al junctions, with an Ag island film on top, separated from the Au electrode by an intermediate MgF_2 film. After this MgF_2–Ag coating, they observed an intensity increase and change of the wavelength dependence of the emission to the Au side. These results may be considered as indication of light emission from the fast mode.

Ag on CaF_2-roughened substrates shows an additional absorption in the range from 360 nm to more than 420 nm depending on the kind of roughness [12]. This absorption corresponds to the high density of states of the fast SPP at the Ag–vacuum boundary of an Ag contact.

The three most often discussed hypotheses for the generation of light in MIM *contacts* are as follows.

(i) Inelastically tunnelling electrons excite the slow mode, which converts into light via surface corrugations [2, 3, 13–20]. This led to the acronym LEIT: light emission by inelastic tunnelling [2].

(ii) Electrons tunnel elastically through the insulating barrier and a fraction of them reach the Ag, Au, Cu–vacuum boundary as hot electrons. There they excite the fast mode, which converts into light via surface corrugations [21–27]. For hot electrons in Ag with an

energy of 2.8 eV above the Fermi energy the electron–electron mean free path is estimated as about 33 nm [28].

(iii) Inelastically tunnelling electrons excite the slow mode, which converts into the fast mode via roughness. Then the fast mode scatters into light at surface corrugations or is converted into light by a prism coupler [29, 9, 16, 17, 10].

Takeuchi *et al* [16] developed a theoretical calculation that dealt with hypothesis (iii). It follows the first-order scattering theory of Laks and Mills [13] but introduces roughness at every boundary of a tunnel junction. It only applies to the case where the slow mode is scattered into the fast mode and the fast mode is converted into light by a prism coupler. These calculations fit the experimental results very well. However this theory cannot be applied to the double scattering of the slow mode into the fast mode and the fast mode into light by surface roughness without a prism coupler.

Sparks *et al* [20] and Ushioda *et al* [30] observed light emission by the slow mode of tunnel junctions with an Au top electrode prepared on microlithographic gratings with periods of 100, 85 and 70 nm and Connolly *et al* [8] presented calculations for this case. However, the intensities emitted into the semispace were only about 8×10^{-8} photons per electron, as inferred by integration over the spatial angle and the photon energy of the emission spectrum in figure 2 of [20], which is at least two orders less than the intensities emitted by our junctions (see below). The maximum emission intensity was in the infrared and not in the range of 620 nm, as observed for Au junctions prepared on CaF_2 substrates (see figure 20).

On the other hand, light-emitting junctions prepared on gratings with 800 nm grating period and prisms map the dispersion relation of the fast mode [21, 30, 16, 17].

The fact that light emission takes place for both bias polarities of the junction [2] seems to support hypothesis (i) or (iii). By assuming an inelastic tunnelling process Davis [31] calculated a higher probability of only about a factor of two that a tunnelling electron excites a surface plasmon when it tunnels into the Ag than when it tunnels into the Al. However, our experimental results show that the observed asymmetry of emission needs a more far-reaching interpretation. Drucker and Hansma [25] showed that tunnel junctions with an Au top electrode can emit electrons into the vacuum for a positive bias of 2.5–3 V. Consequently hot electrons exist in Au tunnel junctions at positive bias and are able to reach the Au–vacuum boundary. We measured the emission of electrons into the vacuum on tunnel junctions with Ag top electrodes (see figure 2).

To test the three hypotheses for rough tunnel junctions we investigated AG, Au, Cu–Al_2O_3–Al contacts not in air, but in ultrahigh vacuum (UHV). We measured the amount of light at both bias polarities [31], observed the light emission also from the Al side of the junction for different top electrode thicknesses, changed the dispersion of the slow mode by varying the thickness of the insulator and covered the Ag surface with O, K and Cs.

2. Experiment [33]

The tunnel junctions were prepared on smooth glass slides, which had been cleaned carefully by boiling them first in diluted sulphuric acid and then in distilled water. After that they were submitted to ultrasonic cleaning in ethanol and then dried under pressure.

The tunnel junctions consisted of a sequence of films: Al 1 mm wide, 30 nm thick, Al_2O_3 covering the whole film 3–4 nm thick and Ag 1.5 mm wide, about 20 nm thick. A schematic representation of the junction is shown in figure 3.

The Al and Al_2O_3 were evaporated in the 10^{-8} mbar range. Then the sample was transferred into the UHV to evaporate the Ag top electrode and investigate the light emission. The Al and Ag were evaporated thermally, the Al_2O_3 with an electron-beam evaporator. The film thicknesses were controlled by a quartz-crystal monitor.

We examined Ag–Al_2O_3–Al tunnel junctions with three types of roughness: (i) nominally smooth junctions, which were evaporated at room temperature directly onto a glass slide, (ii) junctions with a CaF_2 underlayer, which were prepared at room temperature on a 100 nm thick CaF_2 film on top of the glass slide, and (iii) to further increase the density of surface defects of the Ag top electrode, the sample with the CaF_2 underlayer was cooled to about 40 K before preparing the Ag top electrode by evaporation (a so-called cold-deposited film see e.g. [34]). During the experiments the sample was under UHV conditions (5×10^{-10} mbar) and had a temperature of about 40 K.

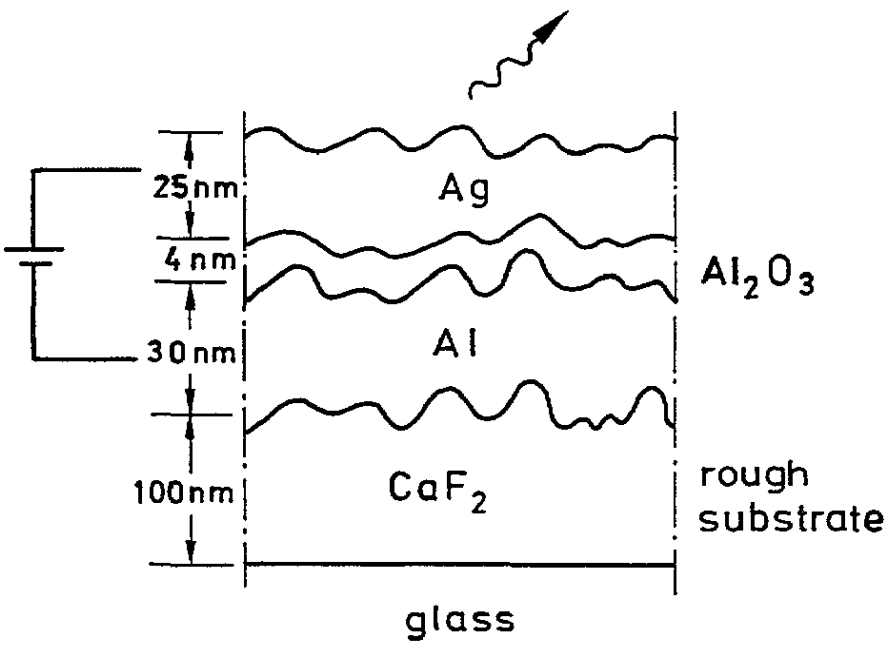

Figure 3. A schematic representation of a tunnel junction with a CaF_2 underlayer.

The emitted light was detected by a spectrograph with a holographic grating, an image intensifier and a diode array. In this way it was possible to receive spectra between 300 and 800 nm in about 1 min. We used glass lenses and Al mirrors to image the sample on the entrance slit of the spectrograph. A schematic representation of the spectrograph is displayed in figure 4.

The spectra are not corrected for the sensitivity given mainly by the image intensifier and the grating. The image intensifier was a proxifier BU2541, which had its best sensitivity below 500 nm [34]. The spectral crosstalking within the proxifier prevented the measurements of accurate cut-offs, which have been well investigated by other authors (see [2], [3] and [10]). Our main interest was the comparison of integral intensities of the emitted light. Typical intensities of the light of the junctions prepared on 100 nm CaF_2 emitted into the semispace at 3.5 V positive bias are about $(5 \pm 2) \times 10^{-5}$ photons

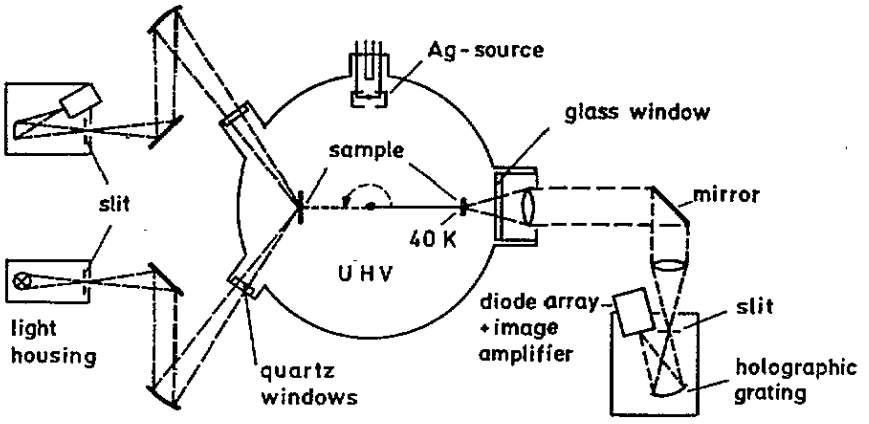

Figure 4. A schematic representation of the optical set-up: reflectivity measurements are made with the left sample position, light emission spectroscopy with the right sample position.

per tunnelling electron. We measured this value by comparing the intensity of a light-emitting junction with the intensity of a 2 mW HeNe laser at 633 nm, which was attenuated appropriately by neutral-density filters.

We also performed reflection measurements in the range between 230 and 840 nm. The light of a deuterium–halogen duplex lamp was focused on the sample and the reflected light was analysed with a spectrograph consisting of a holographic grating and a diode array (see figure 4). This multichannel reflectometer is described in detail in [36].

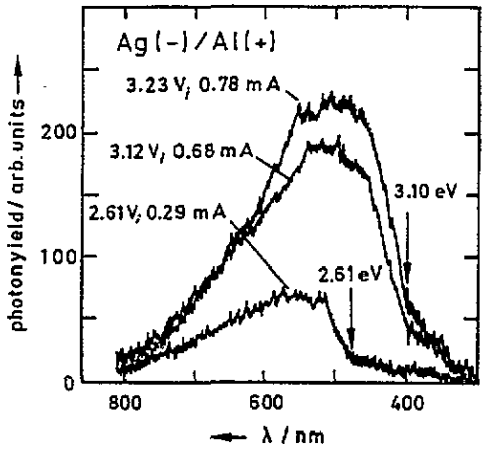

Figure 5. The development of the emitted intensity of a tunnel junction for increasing voltage and current below 3.1 V (electrons tunnel into Al, negative bias). Intensities above the indicated cut-offs are caused by crosstalk within the image intensifier.

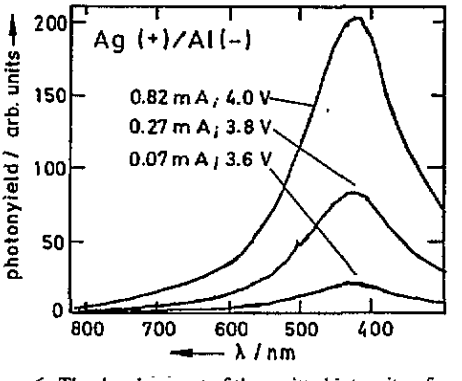

Figure 6. The development of the emitted intensity of a tunnel junction for increasing voltage and current above 3.1 V (electrons tunnel into Ag, positive bias).

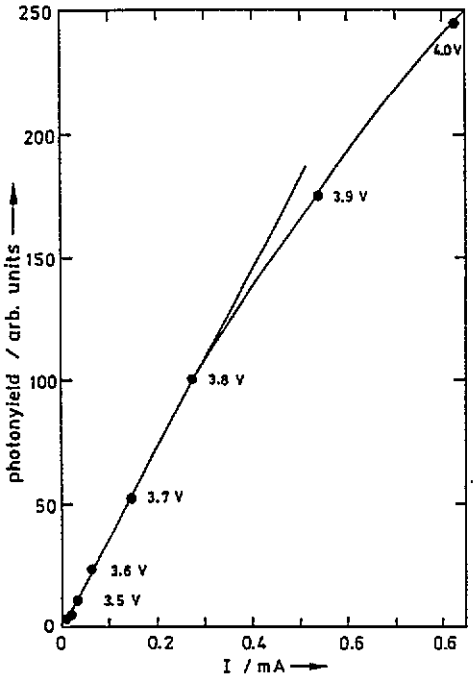

Figure 7. The dependence of the integrated intensity of the tunnel junction from figure 6 on the tunnel current (positive bias).

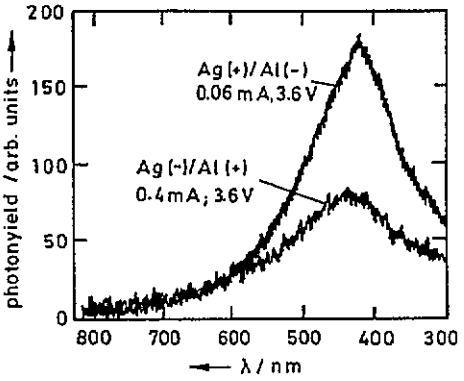

Figure 8. The emitted intensity of one tunnel junction for positive (Ag(+)–Al(−)) and negative (Ag(−)–Al(+)) bias. The difference of the photon yield per electron tunnelling is about a factor of 15.

3. Results and discussion

If not stated otherwise, all junctions have a CaF_2 underlayer of 100 nm thickness. According to [37] the statistical roughness of the CaF_2 films is characterized by a correlation length of about 20 nm and an RMS roughness of about 5 nm.

3.1. Light emission to the vacuum side; dependence on bias

Figures 5, 6 and 7 display some characteristics of the light emission of tunnel junctions with an Ag top electrode. For voltages higher than 3.1 V there is no shift of the wavelength of the maximum intensity observed (see figure 6). The integrated intensity of the emitted light grows linearly with the tunnel current for voltages from 3.1 V to 3.8 V. This is demonstrated in figures 6 and 7 with a tunnel junction at positive bias (i.e. electrons tunnel into the Ag). In this voltage range our junctions have a photon yield per electron independent of the tunnel current and the applied voltage for a given junction.

Figure 8 shows a comparison of spectra of one junction with positive and negative biases. In spite of much higher currents for negative bias the emitted intensity is much higher for positive bias. The photon yield per electron is about 15 times higher when electrons tunnel into the Ag than when they tunnel into the Al. In figure 9 this feature is confirmed for another junction at which increasing voltages were applied with several changes of the bias polarity. For this junction and the junction of figure 13 (just compare the two spectra of the unexposed junction at the top) the photon yield per electron is as much as about 30 times higher for positive bias than for negative bias. Figure 9 gives an

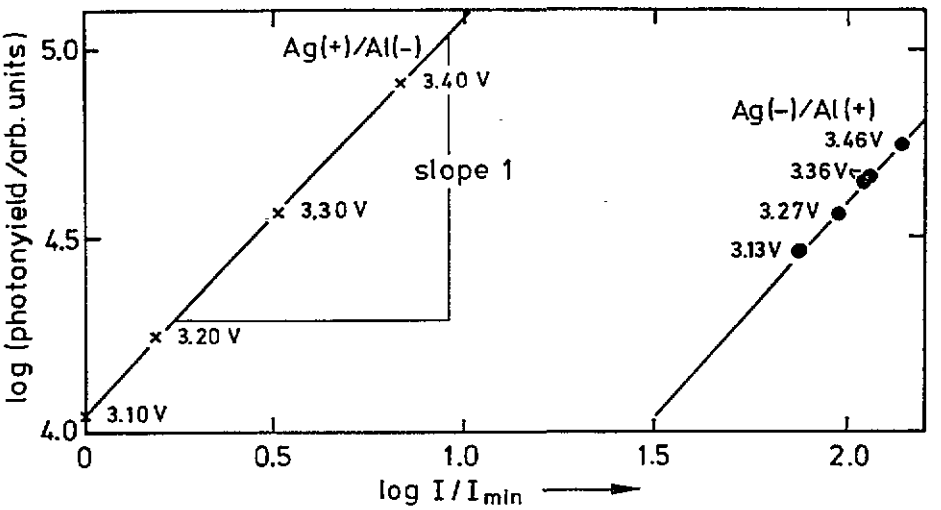

Figure 9. Integrated intensities emitted by one and the same tunnel junction as a function of the current for variations in both polarities and voltages. The intensities depend linearly on the current. The photon yield per electron is about a factor of 30 higher when Ag is positively biased.

indication of the stability of our junctions. The integrated intensities for both bias polarities fit well into the linear dependence on the tunnel current, in spite of several changes of the polarity.

The strong dependence on the polarity of the photon yield per electron is not expected by the calculation of Davis [31] assuming an inelastic tunnelling process. Davis claimed a strong dependence on the polarity of light emission for an injection process which is, in his opinion, the reason why UV emission was observed by Hwang *et al* [38] only with the Al side negatively biased. Dawson and Walmsley [24] and Kroó *et al* [39] observed a two to ten times higher intensity from tunnel junctions when the electrons tunnelled into the top electrode. However, they chose different absolute voltages for the two polarities in order to obtain the same absolute currents. In consequence they calculated, with intensities of different spectral configuration. Lambe and McCarthy [2, 3] and Kirtley *et al* [23] noticed the dependence on the polarity of the intensity, too. Light emission of Si MOS structures with Al contacts [40] exhibits also a dependence on the polarity. In this case there is more intensity when the electrons are injected into the Al than into the Si. Note that the dielectric function of Si has no negative values in the visible region and therefore Si MOS structures have no slow mode as do MIM contacts. Because of the strong dependence of the photon yield per electron on the polarity, we think the fact that light is emitted for both bias polarities is no proof that the origin of the main part of the emitted light is explained by hypothesis (i) or (iii).

3.2. Light emission to the glass side; variation of the Ag film thickness

Figure 10 shows spectra from different tunnel junctions with positive bias observed from the Al side of the junction. The thickness of the Ag top electrode was varied. The top electrodes were prepared on the same bias of CaF_2, Al and Al_2O_3. The Ag film thickness could only be determined by the resistance of the top electrode and the evaporation time. We estimate that in figure 10 $d_1 \simeq 20$ nm, $d_2 \simeq 2d_1$ and $d_3 \simeq 5d_1$. We observed a blue

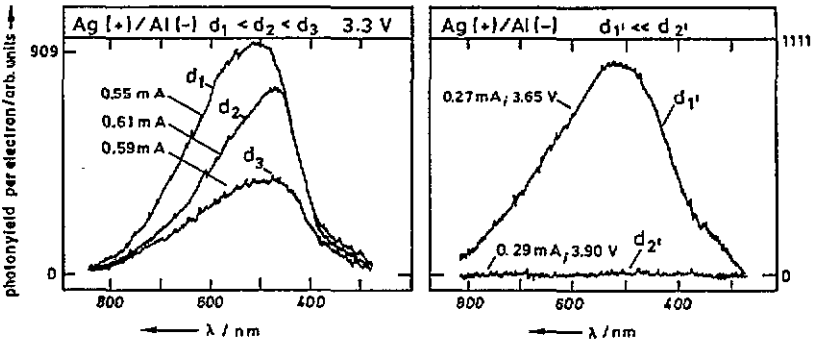

Figure 10. Spectra of two tunnel junctions with positive bias observed from the Al side with different Ag top electrode thicknesses $d_1 < d_2 < d_3$ (first junction, left side, left scale [63]) and $d_1' < d_2'$ (second junction, right side, right scale [63]). $d_1 \sim 20$ nm, $d_2 \sim 40$ nm, $d_3 \sim 100$ nm, $d_1' \sim 20$ nm, $d_s' \sim 400$ nm.

shift of the maximum of the emission and a decrease of the photon yield per electron until the intensity was below the detection limit. Both features indicate that the fast mode is the origin of the observable emitted light. A longer distance of the insulating barrier to the Ag–vacuum boundary suppresses all the possible excitation processes of the fast mode. Light generated at the Ag–vacuum boundary would be extinguished on its way through the Ag. This extinction is dependent on the wavelength. Ag is more transparent for blue than for red light. On the other hand light emitted by scattering of the slow-mode field at the rough Al_2O_3–metal interfaces or some unassigned luminescence within the oxide or from hot electrons traversing these interfaces would not be suppressed by a thick Ag layer—nevertheless it is not observed.

Light emitted by scattering the intermediate SPP at the Al–CaF_2 interface is not expected in the spectral range covered in this work, for the following reason: this process is analogous by the law of optical reciprocity to roughness-mediated absorption by SPPs. Reflection measurements of Al films on CaF_2-roughened substrates show an additional absorption at 140 nm in comparison with a smooth Al film [41]. This absorption concerns the SPP mode at the Al–vacuum boundary. It shifts to about 160 nm when a dielectric overlayer of LiF is evaporated onto the Al [42]. In contrast, Ag films on a CaF_2-roughened substrate display an additional absorption in the visible range [42, 43].

Figure 11 contains spectra for junctions with negative bias and different thicknesses of the Ag top electrode. One observes a decrease in the photon yield per electron, too. The different spectral forms of these spectra are dominated by the difference of the applied voltages. d_1 is about 20 nm and d_2 is much greater, roughly 100 nm [44]. The explanation for the decrease of the photon yield per electron is analogous to that of the decrease at positive bias.

The results presented above correspond to experiments of Dawson *et al* [11], who observed a 30 times higher intensity emitted from the Au side than from the Al side.

In summary, the observable light from a rough junction is emitted by the fast mode.

The variation of light emitted to the Ag side caused by varying the Ag thickness has already been reported by Kirtley *et al* [22]. Since each of the three hypotheses (see section 1) predicts the disappearance at high Ag thickness, we did not repeat this experiment.

3.3. Variation of the oxide thickness

Figure 12 displays spectra of tunnel junctions that differ in the thickness of the insulating

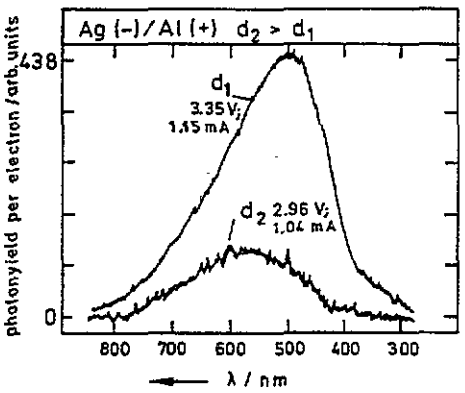

Figure 11. Spectra of tunnel junctions with negative bias observed from the Al side with different Ag top electrode thicknesses d_1, d_2 (see the text) [63].

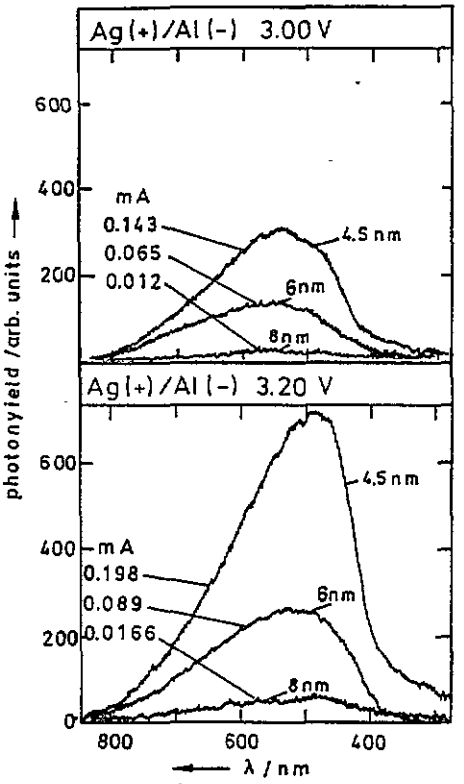

Figure 12. Spectra of tunnel junctions with different insulator thicknesses (see the text).

barrier. The parameters of roughness, Al electrode and Ag top electrode are not changed. No difference in the dependence of the emission intensities on the wavelength is observed for junctions with a thicker insulating barrier. According to Soole and Ager [5], who calculated the dispersion relation and decay length of the slow mode for tunnel junctions with an Ag top electrode for insulator thicknesses of 1, 2, 3 and 4 nm, a blue shift of the emission maximum and an increase of the photon yield per electron with growing insulator thickness are expected if the slow mode contributes significantly to the emission of light. Table 1 gives the integrated photon yield per electron of the spectra in figure 12. The changes of the photon yield per electron are about ±3%, which is in the range of reliability of measurements at different tunnel junctions concerning the adjustment of the optics.

Table 1. Integrated photon yield per electron in arbitrary units of the spectra of figure 12 [63].

d (nm)	3.00 V	3.20 V
4.5	430	684
6	456	642
8	446	669

Watanabe *et al* [17] claim a change of the spectral dependence of the light emission due

to variation of the insulator thickness. However, their claim is based on fitting theoretical calculations to experimental results, and they did not give any indication of a change of their preparation method of the junctions compared. We deposited films of Al_2O_3 with stepped thickness on a 26 mm long Al strip. The thickness of the steps was controlled by a quartz-crystal monitor. In this way the tunnel junctions with different thickness insulator films had the same base of Al and CaF_2-induced roughness. The Ag top-electrode film thickness was kept constant at (25 ± 1) nm.

We conclude that the excitation of the fast mode by conversion of the primary excited slow mode (hypotheses (iii)) does not contribute in a noticeable way.

3.4. Exposure of the Ag surface

Figure 13 displays spectra of one light-emitting Ag junction with, both bias polarities and, additionally, unexposed (top) and exposed (bottom) to the small amount of 5 Langmuir (L) (one L corresponds to the exposure of 10^{-6} Torr s) O_2. In the case of the clean film, the ratio of photon yield per tunnelling electron between positive and negative bias is about 30. One observes a decrease by about 75% in the integrated photon yield per electron when the junction is exposed to a small amount of O_2, as the electrons tunnel into the Ag. In contrast, there is no significant change in the photon yield per electron by exposing the junction to O_2, when the electrons tunnel into the Al [45]. After exposure to O_2, the integrated normalized intensity at positive bias is still about 8.7 times stronger than at negative bias.

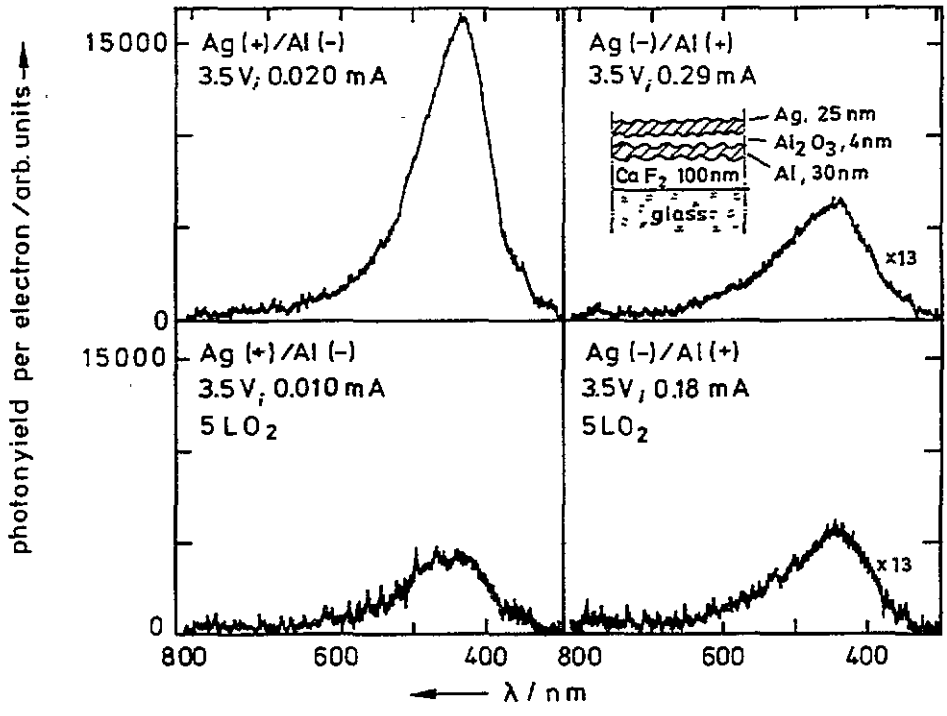

Figure 13. The photon yield per electron of one and the same tunnel junction with an Ag top electrode before and after exposing to 5 L O_2, for both polarities. A significant change in the intensities is only observed when Ag is positively biased. Note that the yields have been multiplied by a factor of 13 for negative bias [63].

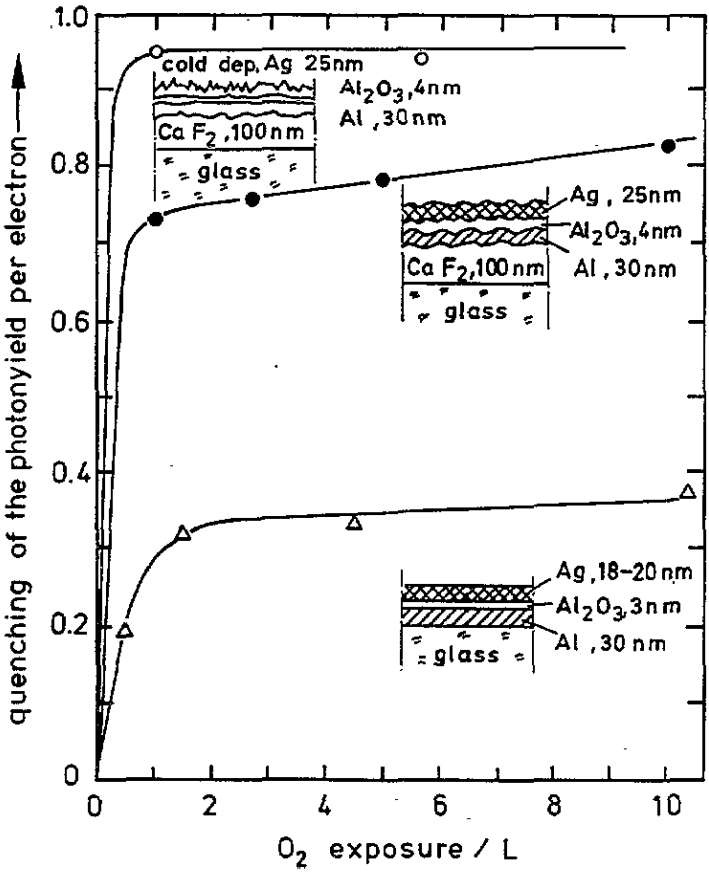

Figure 14. The relative quenching of the photon yield per electron for tunnel junctions prepared differently to change the density of surface defects of the Ag top electrode (see the insets).

It is known that under our experimental conditions O_2 only sticks to defects on the Ag surface in atomic form [46]. The spectra shown in figure 13 are emitted from a junction that was prepared at room temperature on an evaporated 100 mm CaF_2 film. Figure 14 displays the dependence of the relative decrease of the photon yield per electron on O_2 exposure for differently prepared junctions. The absolute photon yield per electron of the 'smooth' junction (see the lowest inset in figure 14) was about a factor of 20 smaller than that for the 'rough' junction (see the middle inset in figure 14), corroborating the result of McCarthy and Lambe [4], whereas the corresponding value for a 'rough' junction with a cold-deposited (40 K) Ag electrode (see the top inset in figure 14) is comparable to that of the smooth junction. We assign this to the loss of a high-quality fast mode at the surface of cold-deposited Ag [47]. For each kind of junction there is a strong decrease for the first 2 L of O_2 exposure. After that the decrease is nearly saturated. For the smoothest contact the photon yield per electron decreases by about 40%, for the contact prepared on a rough CaF_2 film at room temperature it decreases by about 80% and for the contact with the highest defect density of the Ag surface, which was evaporated at 40 K on a junction with a CaF_2 underlayer, it decreases by about 95%. This result corresponds well with the fact that the O only sticks to the surface defects.

In figure 15 reflection measurements of two differently prepared tunnel junctions are

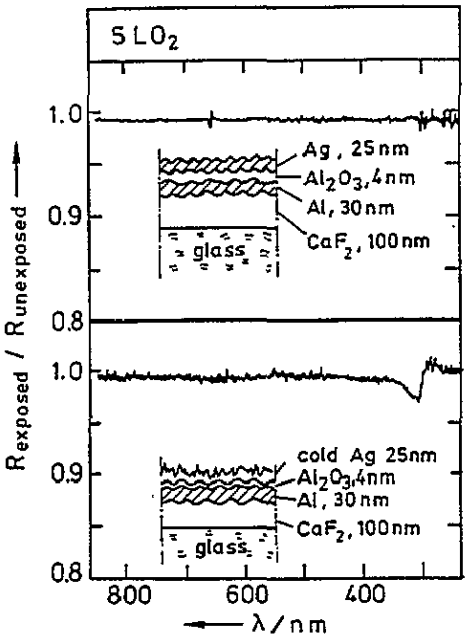

Figure 15. The change of the reflectivity (light is incident from the vacuum side) of tunnel junctions at a positive bias of 3.5 eV due to O deposition, for two differently prepared junctions (see the text).

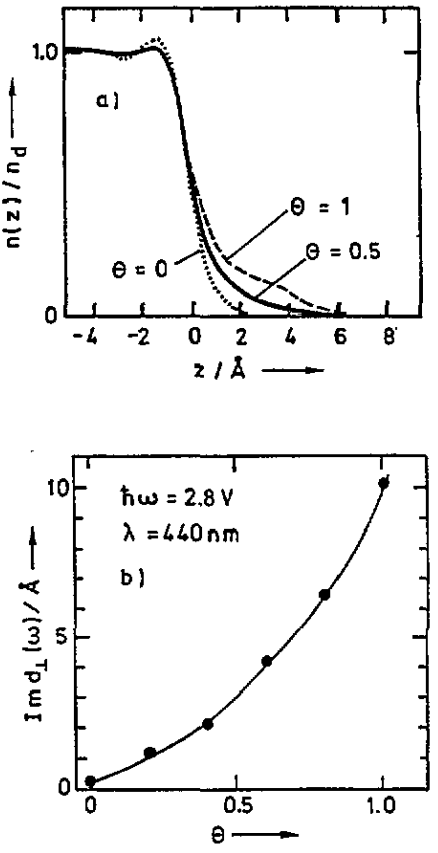

Figure 16. (a) Ground-state electron distributions $n(z)$ for Cs overlayers on Ag at different coverages θ (see the text) (adopted from figure 2 of [56]). z is normal to the surface; the edge of the positive background of 'Ag jellium' is at $z = 0$; $n_d = n(z)$ for from two towards minus infinity. (b) Theoretical calculations of the internal photoemission yield of hot electrons for different Cs coverages on Ag (adopted from figures 1 and 2 of [57]). This yield is proportional to Im $d_\perp(\omega)$. Note that the increase of θ corresponds to an increase of the slow-decaying electron-density tail in (a).

plotted. Both are junctions with a CaF_2 underlayer; they differ in the preparation of the Ag top electrode: one is evaporated at room temperature (top of figure 15) and the other at about 40 K. The curves are the ratio of the reflected light before and after exposing the junction to 5 L O_2. For the less rough Ag surface no change in the reflectivity can be observed. For the cold-deposited Ag film there is only a change in the reflectivity of less than 5% near 327 nm (which corresponds to the plasma frequency of Ag). Because diffuse elastic scattering and inelastic light emission are negligible, the absorption of the samples is given by one minus the reflectivity. The second law of thermodynamics requires detailed balance of emission and absorption for any surface element, for any direction of polarization and any frequency interval [48]. Hence the ratio between emissivity and absorption is independent

of the properties of the sample—this is known as Kirchhoffs law [48]. Therefore, if the absorption is nearly constant after O_2 exposure, so is the emissivity. (Of course, we have extrapolated from the direction of incidence in the reflection experiment to all directions within the space angle of emission subtended by our collection optics.) Therefore, the changes of emission after O_2 exposure up to 95% must be assigned to a change of the source strength of the radiation, and not to a change of emissivity. We come to the same conclusion by the law of optical reciprocity, if we consider the sample as a medium with a local dielectric constant, as used for instance in the problem of Raman scattering from a film coating of an optical grating [49].

Moreover, a change in emissivity would not explain the result that there is a decrease in the photon yield per electron as the electrons tunnel into the Ag, and no change as they tunnel into the Al. Consequently, these result fit neither hypothesis (i) nor (iii). However, the light emission at positive bias can be explained by hypothesis (ii) (see below). Of course, the comparatively weak light emission at negative bias cannot be explained by hot electrons in Ag (hypothesis (ii)), but may be due to weak excitation of the slow mode crosstalking to the fast mode (hypotheses (iii)). However, one cannot exclude a generation of light by hot holes at negative bias, which reach the top electrode–vacuum boundary and excite the fast mode, a mechanism first proposed by Kirtley *et al* [23].

The tunnelling probability of holes is expected to be lower than for electrons. The conduction band of Al_2O_3 is about 8 eV above the valence band [50]. The energetic distance from the Fermi energy to the conduction band is about 2 eV at the Al–Al_2O_3 and about 4 eV at the Al_2O_3–Au interface [51–53]; consequently the valence band is 6 eV below E_F at the Al–Al_2O_3 and 4 eV at the Al_2O_3–Au interface. (No data are known to us for the Al_2O_3–Ag interface.) Nevertheless, tunnelling of holes up to the outside Ag surface is demonstrated in [54].

4. The hypothesis of enhanced electron–photon coupling at rough surfaces [1]

A theoretical approach to the decrease of the electron–photon coupling caused by O_2 may be based on the explanation by Liebsch [55] of the enhancement of optical second-harmonic generation (SHG) after covering smooth Ag (characterized by a jellium with the 5 sp electron density of Ag) by submonolayers of alkali metals (characterized by a slab of the thickness of one monolayer of Cs with electron density $n_{bulk}(\text{alkali})\theta$, with surface concentration of Cs θ 1 at monolayer coverage). Alkali metals on Ag induce an extended tail of the ground-state electron density in front of the Ag surface [56] (see figure 16(a)). This effect caused besides an increase of the non-linear response also an increase of the linear surface electron–photon coupling characterized by Im $d_\perp(\omega)$. In [57] the theoretical result displayed in figure 16(b) is meant to describe internal photoemission of hot electrons (for photon energies below the work function of alkali-covered Ag). Here we use the result in its time-reversed form as inverse photoemission by hot electrons. The corresponding theoretical results on photoemission into the vacuum were confirmed by measurements of the photoemission of Ag on which Cs was deposited [57]. The theoretical ratio of the electron yields for p- to s-polarized light has a resonance-like structure around 2 eV (617 nm) with a maximum of about 20 when Ag is covered with less than 1 ML of Cs. We think that atomic defects and open planes on silver surfaces are sites where the tail of the electron-density profile protrudes further out from the surface than from the low-index Ag surfaces [58]. We postulate that at these active sites the electron–photon coupling is increased. O_2 (adsorbed at defects) passivates the active sites by transferring electrons near the Fermi level from the

defected region into the localized O 2p orbitals, 2.9 eV below the Fermi level, as observed by photoemission measurements [59, 60], thus rendering the electron profile steeper. We assign most of the emitted light at positive bias, which is not quenched by O_2 (see figure 14) to 'unenhanced' hot-electron–photon coupling at low-index facets of Ag. An assignment to hypotheses (iii) is unlikely, because the normalized emission after 'O_2 quenching' at positive bias is about one order of magnitude higher than that at negative bias. A theoretical test of our postulation of enhanced electron–photon coupling at atomically rough Ag, Cu or Au surfaces is not yet available—so far, only calculations of static screening at stepped jellium surfaces have been published [61]. From the calculations of Liebsch *et al* [57] it is expected that the deposition of K or Cs on the surface of the Ag top electrode increases the photon yield per electron of a tunnel junction. This is confirmed by the results in figures 17 and 18. About 1 mL of either material enhances the emission almost threefold.

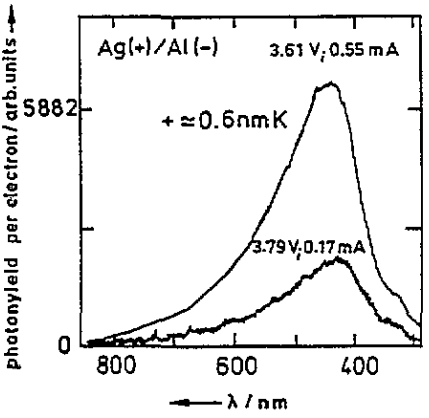

Figure 17. The photon yield per electron of a tunnel junction with an Ag top electrode before and after deposition of 0.6 nm K [63].

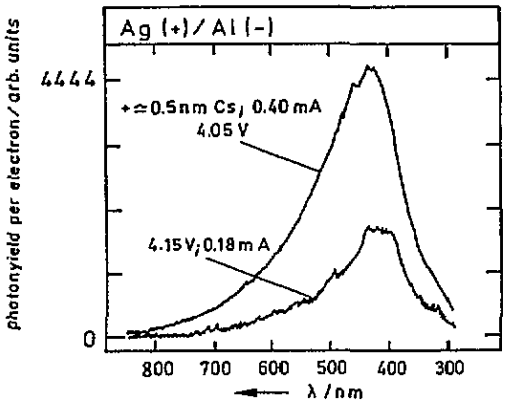

Figure 18. The photon yield per electron of a tunnel junction with an Ag top electrode before and after deposition of 0.5 nm Cs [63].

There should be a decrease of the photon yield per electron at tunnel junctions with Cu top electrodes on exposure to O_2, too. In figure 19 spectra of one tunnel junction with a Cu top electrode are displayed. On exposing the junction to O_2 a similar effect as for a junction with an Ag top electrode is observed. The same holds true for junctions with Au top electrodes, as shown in figure 20. The decrease of the photon yield per electron does not correspond to an experiment performed by Sparks and Rutledge [18]. They evaporated an additional film of Ge on Au–Al_2O_3–Al contacts and found that there was only a negligible change in the emission characteristic of their junctions in spite of the fact that the fast mode was quenched due to the Ge overlayer. However, they investigated their samples at room temperature and had problems with the stability of their junctions. Furthermore, they did not work under vacuum conditions, so the Au surfaces of their samples were polluted with O.

5. Enhanced electron–photon coupling [1] and surface-enhanced Raman scattering (SERS)

The light emission at positive bias observed in this work is assigned to inverse photoemission by hot electrons, enhanced at sites of atomic-scale roughness, whose microscopic nature has

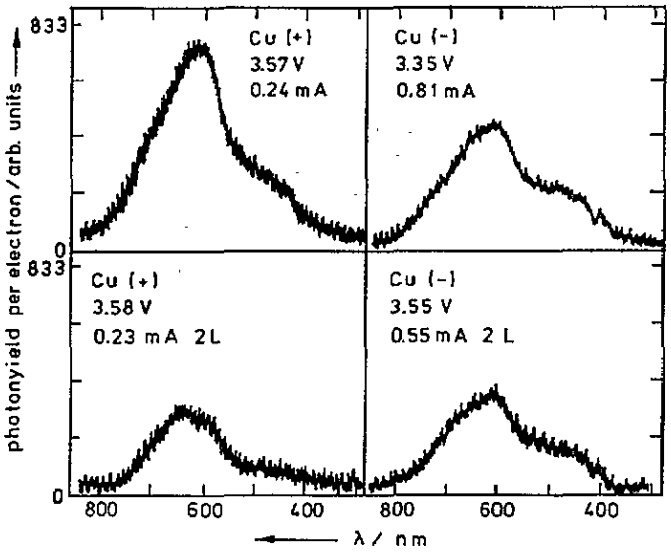

Figure 19. The photon yield per electron of a tunnel junction with a Cu top electrode before and after exposing to 2 L O_2, for both polarities. A significant change in the intensities is only observed when Ag is positively biased [63].

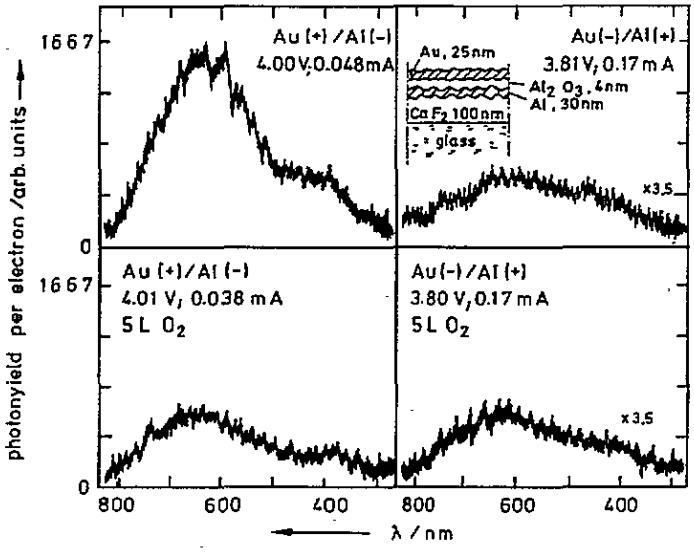

Figure 20. The photon yield per electron of a tunnel junction with an Au top electrode before and after exposing to 5 L O_2, for both polarities. A significant change in the intensities is only observed when Ag is positively biased [63].

not yet been clarified. In detail, this process involves tunnelling of electrons into the Ag top electrode, a fraction of which reach the Ag–vacuum interface as hot electrons. Preferentially at sites of atomic-scale roughness, the hot electrons interact with the electromagnetic field in the vacuum. Preferentially, this is the field of the fast SPPs. The fast SPPs are excited

by transitions of the hot electrons into states near the Fermi energy. The SPPs in turn are scattered into radiative modes by the roughness of the surface, imposed by the underlying CaF_2 film.

Of course, the time-inverted process, enhanced photoemission of hot electrons, would exist as well. At smooth surfaces this enhancement by varying the electron density profile is predicted by theory [57], (see figure 16).

A review article on surface-enhanced Raman scattering (SERS) [62] proposed a Raman-scattering process, involving both these enhanced electron–photon interaction mechanisms and temporary charge transfer to orbitals of adsorbates, in order to account for the short-range, chemically specific and vibrationally selective enhancement of the Raman scattering by adsorbate vibrations, and the quenching of this enhancement by O_2. This SERS mechanism is further supported by the conclusions of this work.

6. Summary

Light-emitting MIM tunnelling junctions on a rough substrate, with Ag top electrodes, were prepared and investigated for the first time in UHV at 40 K.

We measured the emission spectra and the integrated intensity at both bias polarities, observed the light emission also from the Al side of the junction for different Ag electrode thicknesses, changed the thickness of the Al_2O_3 insulator layer and covered the Ag surface by controlled exposure to O_2, K or Cs. In this way we discriminated between emission from the fast, intermediate and slow surface plasmon polaritons. Observable light in both directions of emission is only emitted by the fast mode. Changing the dispersion relation of the slow mode by variation of the thickness of the insulator layer changes neither the spectral distribution nor the photon yield per tunnelling electron. We conclude that for rough junctions the contribution to light emission by crosstalking of the slow mode with the fast mode is negligible.

The differences in photon yield per tunnelling electron at the same absolute tunnel voltages but opposite polarities are given by factors of about 30, the higher ratio oberved for emission by electrons tunnelling into Ag (positive bias). This is assigned to Kirtley *et al* 's hot-electron mechanism [26]. It is corroborated by quenching of the light emission by O_2 (but only at positive bias) without changes of the optical reflectivity in the visible range above 2%.

The coupling of hot electrons to the fast mode at rough tunnel junctions, and the 'O_2 quenching', are explained with the help of Liebsch's model of electron–photon coupling [1] within the inhomogeneous electron gas at jellium–vacuum surfaces [57], postulating enhanced coupling and oxygen quenching at sites of atomic-scale roughness. The light emitted by the fast mode after O_2 quenching at positive bias is assigned to 'unenhanced' electron–photon-coupling [1] the relatively weak light emission at negative bias may perhaps be due to to coupling of the fast mode with hot holes, but 'crosstalk' of the slow mode to the fast mode cannot be excluded in this case.

The consequences of increased hot-electron–photon coupling [1] in Raman scattering from adsorbates on free-electron metals have been described in [62].

References

[1] By electron–photon coupling we mean both electron–hole pair excitation by light and the respective matrix elements either in the semiclassical theory of interaction of electromagnetic waves with the electrons

or of one-photon processes in second quantization. The same expression is used for the time reversed processes. Surface plasmon polaritons (SPPs) are 'photons bound to surfaces'—the respective coupling is called electron–photon coupling as well.

[2] Lambe J and McCarthy S L 1976 *Phys. Rev. Lett.* **37** 923
[3] McCarthy S L and Lambe J 1977 *Appl. Phys. Lett.* **30** 427
[4] Soole J B D and Hughes H P 1988 *Surf. Sci.* **197** 250
[5] Soole J B D and Ager C D 1989 *J. Appl. Phys.* **65** 1133
[6] Kurdi B N and Hall D G 1984 *Opt. Commun.* **51** 303
[7] Kurdi B N and Hall D G 1986 *Phys. Rev.* B **34** 3980
[8] Connolly M P, Whitaker M A B and Dawson P 1992 *Appl. Phys. Lett.* **61** 2776
[9] Pierce R M, Rutledge J E and Ushioda S 1987 *Phys. Rev.* B **36** 1803
[10] Suzuki C, Watanabe J, Takeuchi A, Uehara Y and Ushioda S 1989 *Solid State Commun.* **69** 35
[11] Dawson P, Ferguson A J L and Walmsley D G 1982 *Solid State Commun.* **44** 1127
[12] Stanford J L, Bennett H E, Bennett J M, Ashley E J and Arakawa E T 1968 *Bull. Am. Phys. Soc.* **13** 989
[13] Laks B and Mills D L 1979 *Phys. Rev.* B **20** 4962
[14] Laks B and Mills D L 1980 *Phys. Rev.* B **21** 5175
[15] Parvin K and Parker W 1981 *Solid State Commun.* **37** 629
[16] Takeuchi A, Watanabe J, Uehara Y and Ushioda S 1988 *Phys. Rev.* B **38** 12948
[17] Watanabe J, Takeuchi A, Uehara Y and Ushioda S 1988 *Phys. Rev.* B **38** 12959
[18] Sparks P D and Rutledge J E 1989 *Phys. Rev.* B **40** 7574
[19] Ushioda S 1991 *J. Lumin.* **47** 131
[20] Sparks P D, Sjodin T, Reed B W and Stege J 1992 *Phys. Rev. Lett.* **68** 2688
[21] Kirtley R J, Theiss T N and Tsang J C 1980 *Appl. Phys. Lett.* **37** 435
[22] Kirtley R J, Theiss T N and Tsang J C 1981 *Phys. Rev.* B **24** 5650
[23] Kirtley R J, Theiss T N, Tsang J C and DiMaria D J 1983 *Phys. Rev.* B **27** 4601
[24] Dawson P and Walmsley D G 1986 *Surf. Sci.* **171** 135
[25] Drucker J and Hansma P K 1984 *Phys. Rev.* B **30** 4348
[26] Kirtley J R, Theiss T N, DiMaria D J, Tsang J C, Fischetti M V and Brorson S D 1985 *Dynamical Phenomena at Surfaces, Interfaces and Superlattices* ed F Nizzoli, K-H Rieder and R F Willis (Berlin: Springer)
[27] Dawson P, Walmsley D G, Quinn H A and Ferguson A J L 1984 *Phys. Rev.* B **22** 3164
[28] Kanter H 1970 *Phys. Rev.* B **1** 522
[29] Ushioda S, Rutledge J E and Pierce R M 1985 *Phys. Rev. Lett.* **54** 224
[30] Ushioda S, Uehara Y, Takada M, Otsubo K and Murota J 1992 *Japan. J. Appl. Phys.* **31** L870
[31] Davis L C 1977 *Phys. Rev.* B **16** 2482
[32] MIM contracts are much more susceptible to breakdown (transformation into a low-resistivity contact) at negative bias (electrons tunnelling into Al), for a yet unknown reasons. Therefore, many previous reports are only on results of positive bias.
[33] Hänisch M *Dissertation* Heinrich-Heine-Universität Düsseldorf, Fortschrittsberichte VDI, Reihe 9, Nr. 186
[34] Otto A 1988 *Indian J. Pure Appl. Phys.* **26** 141
[35] Cromwell R H, Strittmatter P A, Allen R G, Hege E K, Kühr H, Marien K-H, Funk H W and Frank K 1985 *Ad. Electron. Electron Phys.* A **64** 77
[36] Hänisch M and Otto A 1991 *J. Electroanal. Chem.* **308** 113
[37] Varnier F, Mayani N and Rasigni G 1989 *Appl. Opt.* **28** 127
[38] Hwang T-L, Schwarz S E and Jain R K 1976 *Phys. Rev. Lett.* **36** 379
[39] Kroó N, Szentirmay Z S and Félserfalvi J 1986 *Opt. Commun.* **36** 345
[40] Watanabe J, Uehara Y, Murota J and Ushioda S 1993 *J. Appl. Phys.* **32** 99
[41] Feuerbacher B P and Steinmann W 1969 *Opt. Commun.* **1** 81
[42] Stanford J L 1970 *J. Opt. Soc. Am.* **60** 49
[43] Schröder E 1969 *Opt. Commun.* **1** 13
[44] As in the case of positive bias, we tried to extinguish light emission to the glass side by even thicker Ag films—but in every case the contract broke down, for as yet unknown reasons (see also [34]). Of course, we cannot exclude the possibility that the light is not extinguished due to a hot-electron mechanism at the Al–substrate interface, but we think this is unlikely for the reasons presented above.
[45] Note that there is an unexplained change of the tunnel current due to O_2 exposure. Changes of the tunnel characteristics were also observed by Drucker and Hansma, who deposited small amounts of Cs on the top electrode of their junction [26]. Of course, the current change was considered in our calculations of the photon yield per electron.
[46] Campbell C T 1985 *Surf. Sci.* **157** 43
[47] Reed C E, Giergiel J, Ushioda S and Hemminger J C 1985 *Phys. Rev.* B **31** 1873

[48] Reif F 1985 *Statistische Physik und Theorie der Wärme* (Berlin: de Gruyter) ch 9.15
[49] Arnold M, Bussemer P, Hehl K, Grabhorn H and Otto A 1992 *J. Mod. Opt.* **39** 2329
[50] Arakawa E T and Williams M W 1968 *J. Phys. Solids* **29** 735
[51] Pollack S R and Morris C E 1964 *J. Appl. Phys.* **35** 1503
[52] Mosatov A L 1968 *Sov. Phys.–Solid State* **9** 2580
[53] Burshtein Z and Livinson J 1975 *Phys. Rev.* B **12** 3453
[54] Diesing D, Janssen H and Otto A 1994 *ECOSS XIV* submitted
[55] Liebsch A 1989 *Phys. Rev.* B **40** 3421
[56] Liebsch A, Hincelin G and Lopez-Rios T 1990 *Phys. Rev.* B **41** 10463
[57] Liebsch A, Benemanskaya G V and Lapushkin M N 1994 *Surf. Sci.* **302** 303
[58] Smoluchowski R 1941 *Phys. Rev.* **60** 661
[59] Eickmans J, Goldmann A and Otto A 1983 *Surf. Sci.* **127** 153
[60] Eickmans J, Otto A and Goldmann A 1985 *Surf. Sci.* **149** 293
[61] Ishida H and Liebsch A 1993 *Surf. Sci.* **297** 106
[62] Otto A, Mrozek I, Grabhorn H and Akemann W 1992 *J. Phys.: Condens. Matter* **4** 1143
[63] The arbitrary units are counts per channel within 60 s divided by the tunnelling current, in milliamperes. Note that the photon yield per electron from different MIM contacts may vary within a factor of up to ten at the same tunnel voltage.